ACS Medicinal Chemistry Letters

pubs.acs.org/acsmedchemlett

Letter

Insight on Some Newly Synthesized Trisubstituted Imidazolinones as VEGFR-2 Inhibitors

Manar R. Mohamed, Walaa R. Mahmoud,* Rana H. Refaey,* Riham F. George, and Hanan H. Georgey

Cite This: ACS Med. Chem. Lett. 2024, 15, 892−898

Read Online

ACCESS | Metrics & More | Article Recommendations | Supporting Information

ABSTRACT: Two series of ten new 1,2,4-trisubstituted imidazolin-5-ones were synthesized and screened against MCF-7 breast cancer and A549 lung cancer cell lines to test their potential in vitro anticancer activity. The results revealed preferential activity of the tested compounds toward MCF-7 cell lines compared to A549 cell lines. The most promising ten compounds (**3a**, **3c**, **3f**, **3g**, **3h**, **3i**, **3j**, **6a**, **6f**, and **6i**) were subjected to VEGFR-2 enzyme inhibitory activity testing to further explore their mechanism of action. The tested compounds showed remarkable enzyme inhibition in micromolar concentrations ranging from 0.07 to 0.36 μM, compared with Sorafenib and Sunitinib with IC_{50} values of 0.06 and 0.12 μM, respectively. The most promising candidate, **3j**, was further evaluated for its cell cycle phases, apoptotic induction ability, as well as its antiproliferative activity and inhibitory potential for endothelial cell migration, analyzed by a cell scratch assay. Furthermore, in silico studies were also performed to identify and detect the stability of the binding poses.

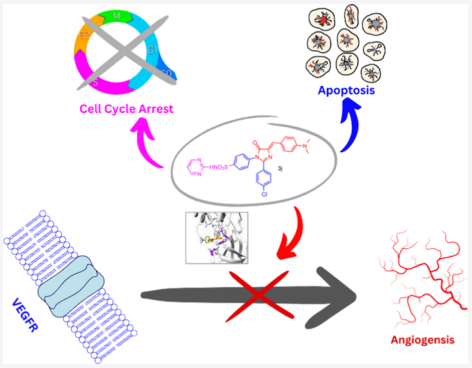

KEYWORDS: *Imidazolinones, Anticancer, VEGFR-2 inhibitors, Molecular dynamics*

Kinases are proteins that covalently attach phosphates to other proteins at specific residues in order to regulate their biological activity. They are divided into two primary categories; serine/threonine kinases and tyrosine kinases.[1] It has been demonstrated that the vascular endothelial growth factor VEGF-A and its receptors VEGFR-1 and VEGFR-2 are necessary in both physiologic and pathologic angiogenesis.[2−4] Many factors influence the pathological angiogenesis seen in cancer cells, such as oncogene expression, variable growth factors, a variety of cytokines, and hypoxia. These factors all up-regulate VEGF expression, which in turn promotes endothelial cell growth and cell migration and inhibits programmed cell death.[5] Sorafenib (**I**) and Lenvatinib (**II**) are type-II VEGFR-2 inhibitors that are currently used for the treatment of several cancers with promising outcomes. They both share common pharmacophoric features which are required for VEGFR-2 binding: a heterocycle "head" that occupies the adenine region in the ATP binding pocket and carries H-bond donor and/or acceptor groups, a "linker" that extends over the gatekeeper residue, as well as a hydrogen-bonding moiety and a hydrophobic moiety "tail" that occupies the allosteric pocket (Figure 1).[6] Hence, the development of similar small molecule inhibitors is still a beneficial strategy in developing newer cancer treatments.

Several substituted imidazolinone derivatives have reported pronounced anticancer activity via VEGFR-2 inhibition such as the 2-thioxoimidazolidin-4-ones **III** and **IV** with IC_{50} values of 25.14 and 19.78 nM, respectively, compared to Sorafenib (IC_{50} = 35.62 nM),[7] as well as **V** with 10-fold greater selectivity against VEGFR-2 (IC_{50} = 0.043 μM) over VEGFR-1 (IC_{50} = 0.51 μM), compared to Vatalanib (IC_{50} = 0.054 and 0.14 μM, respectively).[8] Similarly, compounds **VIa,b** showed remarkable cytotoxic activity, with IC_{50} values of 18.0 and 17.8 μg/mL against MCF-7, as well as IC_{50}s of 10.9 and 12.3 μg/mL against HepG2, respectively, compared to vinblastine (IC_{50} values of 6.1 and 4.6 μg/mL, respectively).[9] Likewise, compounds **VIIa,b** resulted in an increase in the percentage of apoptotic cells to more than 40% and more than 30%, respectively, than the control non-treated cells under investigation.[10] Furthermore, substitution by a 4-dimethylamino group yielded more potent compounds with greater IC_{50} values against colorectal HCT-116 and HeLa cells as compound **VIII**[11] (Figure 2). Moreover, the presence of a sulfonamide moiety had a positive impact on the in vitro anticancer activity of many promising compounds.[12−14] Consequently, the scaffold design of the VEGFR-2 inhibitor target compounds was based on combining the substituted imidazolone head (red) with a phenyl linker (green) and sulfamoyl moiety as the H-bonding moiety (purple) in addition to a tail moiety (blue) (Figure 2).

Received: February 27, 2024
Revised: May 17, 2024
Accepted: May 24, 2024
Published: May 29, 2024

https://doi.org/10.1021/acsmedchemlett.4c00095
ACS Med. Chem. Lett. 2024, 15, 892−898

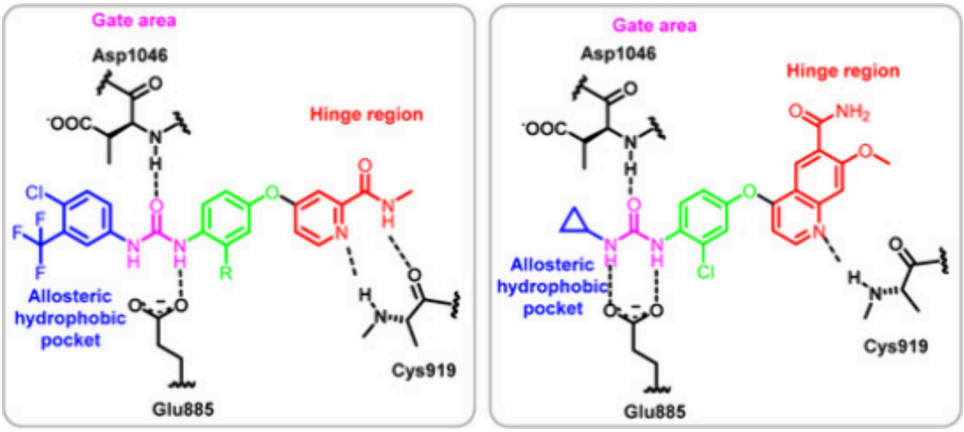

Figure 1. Representation of Sorafenib (**I**) and Lenvatinib (**II**) in the VEGFR-2 active site.[6]

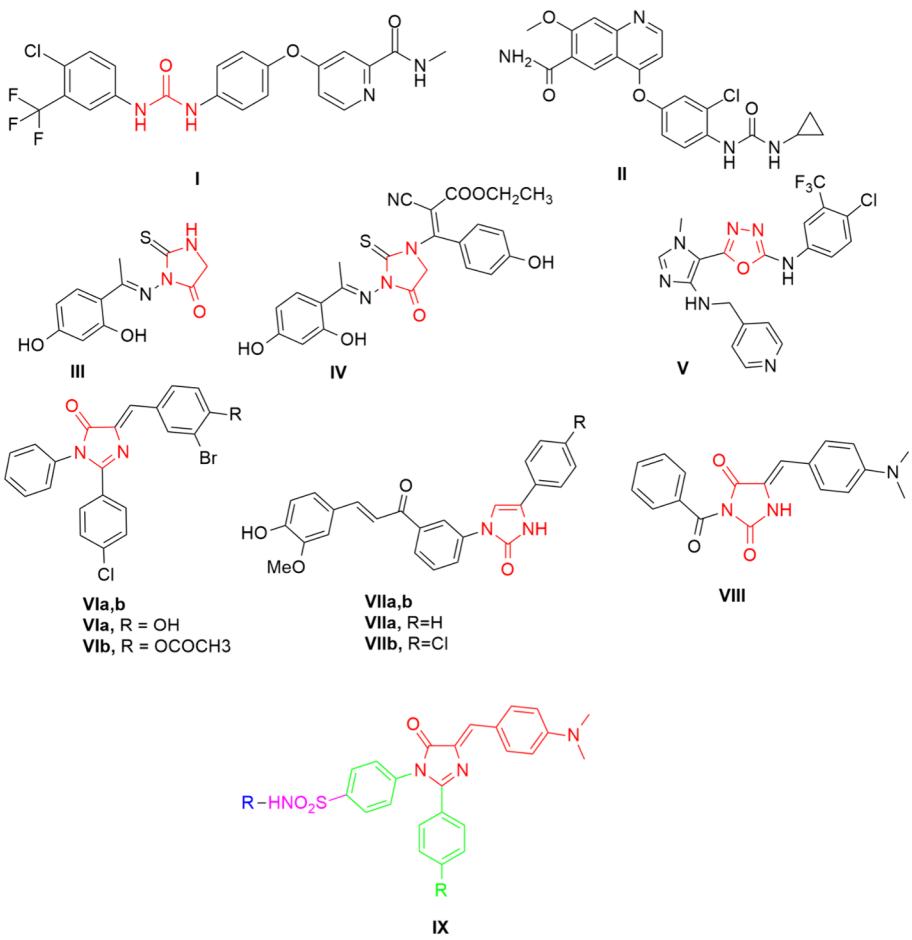

Figure 2. Structures of some VEGFR-2 inhibitors (**I**–**VIII**) and design approach to novel 1,2,4-trisubstituted imidazolinone-derivative VEGFR-2 inhibitors (**IX**).

Therefore, based on a hybridization approach, modifications, including linker elongation between the imidazolinone and the benzenesulfonamide moiety via an amino-2-oxoethyl benzoate spacer to produce compounds **6a**–**j**, were proposed in order to obtain new derivatives with enhanced anticancer activity. The target compounds **3a**–**j** and **6a**–**j** were synthesized according to the procedures outlined in Schemes 1 and 2. In Scheme 1, benzoyl glycines **1a**,**b** were synthesized according to the reported method[15,16] and were then cyclized via Erlenmeyer's method into the corresponding 2,4-disubstituted oxazolones **2a**,**b**.[17,18] Finally, imidazolin-5-one derivatives **3a**–**j** were furnished through the reaction of oxazolone intermediates **2a**,**b** with different sulfonamide derivatives in glacial acetic acid in the presence of anhydrous sodium acetate. The IR spectra revealed the disappearance of the characteristic C═O band of oxazolone at 1762–1766 cm^{-1} and the appearance of a new C═O band of the imidazolone at 1701–1662 cm^{-1}, along with the appearance of an NH band at 3356–3224 cm^{-1} and two stretching bands at 1377–1315 cm^{-1} and 1195–1145 cm^{-1}, which confirmed the introduction of the sulfonamide

https://doi.org/10.1021/acsmedchemlett.4c00095
ACS Med. Chem. Lett. 2024, 15, 892–898

Scheme 1. Synthesis of Compounds 3a−j[a]

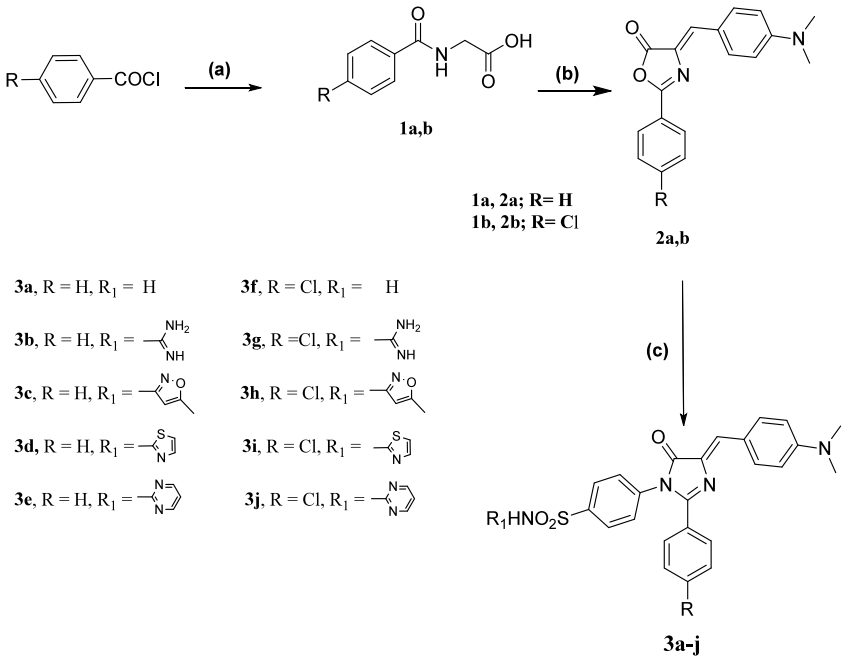

[a]Reagents and reaction conditions: (a) Glycine, 10% NaOH, 2 h, rt. (b) 4-Dimethylamino benzaldehyde, fused sodium acetate, acetic anhydride, 2 h, W.B, 100 °C. (c) Un/substituted sulfonamides, glacial acetic acid, fused sodium acetate, 8 h, W.B, 100 °C.

Scheme 2. Synthesis of Compounds 6a−j[a]

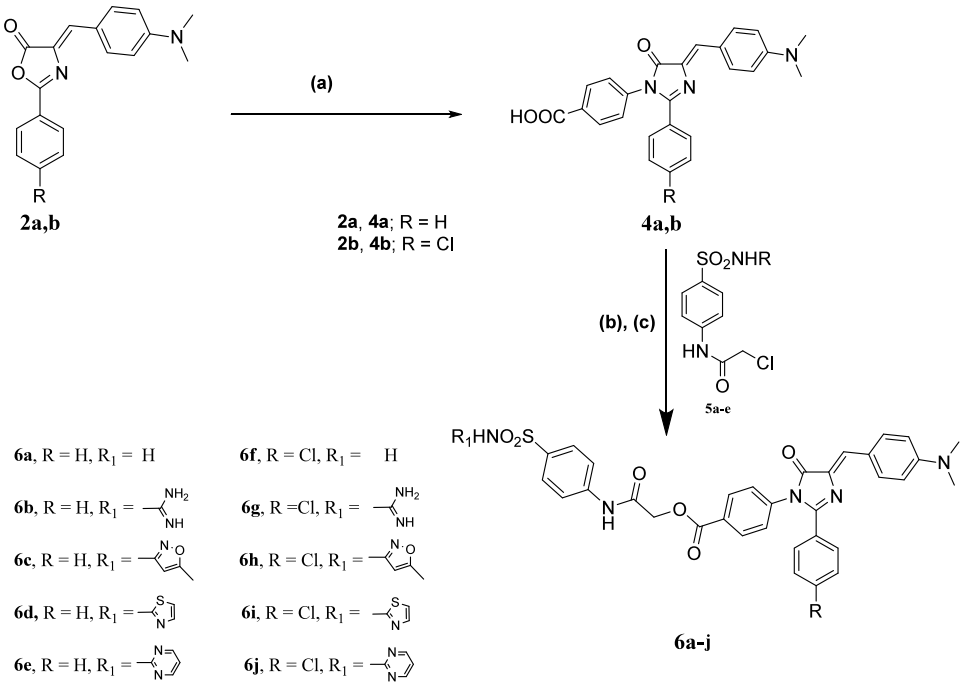

[a]Reagents and reaction conditions: (a) Amino benzoic acid, fused sodium acetate, 8 h, W.B, 100° C. (b) Alcoholic NaOH solution. (c) Chloroacetamido sulfonamides (**5a−e**), dry DMF, 4 h, 100° C.

moiety. Additionally, the ^{1}H NMR spectra of compounds **3c** and **3h** revealed a singlet signal at 2.31 and 2.08 ppm, respectively, for the CH_3 group and the appearance of a characteristic signal integrated for one proton at 6.14 and 6.12 ppm corresponding to the H_4 proton of the oxazole ring. In Scheme 2, intermediates **2a,b** were reacted with 4-amino benzoic acid into the corresponding imidazolinones **4a,b** as reported,[19] followed by the formation of sodium salt through the addition of alcoholic sodium hydroxide. The sodium salts of the acids were then reacted with the chloracetamido sulfonamides **5a−e**[20−22] to obtain the target final esters **6a−j**. The IR spectra of the ester derivatives revealed the appearance of two additional C═O bands, one for the ester group (1701−1685 cm^{-1}) and the other for the amide group (1651−1597

https://doi.org/10.1021/acsmedchemlett.4c00095
ACS Med. Chem. Lett. 2024, 15, 892−898

cm^{-1}). Additionally, the disappearance of the stretching band corresponding to the COOH group as well as the appearance of two stretching bands of the SO_2 group at 1315 cm^{-1} and 1168−1161 cm^{-1} were observed. The ^1H NMR spectrum revealed the presence of a singlet signal at 4.97−4.77 ppm integrated for the two protons corresponding to the CH_2 group. Compounds **6c** and **6h** showed an additional signal at 6.12 and 6.07 ppm, respectively, corresponding to the CH proton of the oxazole ring and a singlet signal at 2.29 and 2.26 ppm, respectively, corresponding to the aliphatic CH_3 group.

The 20 newly synthesized compounds were subjected to in vitro cytotoxic activity against two cancer lines, namely, human breast (MCF-7) and lung (A549) cancer cell lines. The IC_{50} values of the tested compounds compared to two reference drugs (Sorafenib and Doxorubicin, in μM concentration) are summarized in Table 1. A detailed look at the results indicates

Table 1. IC_{50} Values in μM of the Newly Synthesized Compounds against MCF7 and A549 Cell Lines and the Ten Most Active Compounds against VEGFR-2 Kinase Enzyme Using the Reference Drugs

	In vitro cytotoxicity IC_{50} (μM)[a]		In vitro inhibition IC_{50} (μM)[a]
Compound	MCF-7	A549	VEGFR-2
3a	19.53	29.03	0.20
3b	37.42	61.16	NT
3c	9.85	10.07	0.14
3d	39.89	31.55	NT
3e	21.06	29.56	NT
3f	11.51	28.83	0.10
3g	13.55	27.81	0.16
3h	11.50	42.36	0.11
3i	8.65	16.17	0.10
3j	5.86	7.66	0.07
6a	17.65	14.13	0.02
6b	27.71	38.66	NT
6c	26.81	30.55	NT
6d	26.52	16.65	NT
6e	28.82	27.34	NT
6f	24.23	25.00	0.36
6g	17.19	20.16	NT
6h	42.13	45.45	NT
6i	10.03	12.91	0.11
6j	28.37	58.01	NT
Sorafenib	4.88	7.46	0.06
Doxorubicin	6.521	4.985	–
Sunitinib	–	–	0.12

[a]Data are presented as mean of the IC_{50} values from three different experiments. **NT** = not tested.

that the compounds generally revealed better activity toward MCF-7 (IC_{50} = 5.86−19.53 μM) than A549 (IC_{50} = 7.46−61.16 μM). Compound **3j** with a 1-sulfadiazinyl moiety was the most active compound with an IC_{50} value of 5.86 μM on the MCF-7 cell line, compared to an IC_{50} value of 6.52 μM for Doxorubicin. The in vitro activity revealed that the *N*-substitution by a methoxazole ring in compound **3c** and thiazole ring in compounds **3i** and **6i** showed considerable activity against the MCF7 cell line with IC_{50} values of 9.85, 8.65, and 10.03 μM, respectively. The 4-chloro phenyl derivatives **3f**, **3g**, and **3h** were found to have moderate activity with IC_{50} values of 11.51, 13.55, and 11.50 μM, respectively.

The most active compound, **3j**, was further assessed in vitro against the human normal cell line WI-38 to measure its selectivity index (SI; Table 2). The results reveal that compound **3j** has a higher selectivity toward the cancer cell lines compared to the normal one, which is indicative of its relative safety.

Table 2. Selectivity Index (SI) of Compound 3j

ID	IC_{50} (μM)	SI[a]
3j/MCF-7	5.86	3.69
3j/A549	7.66	2.88
3j/WI-38	21.63	–

[a]IC_{50} of the tested compounds against the normal cell line WI-38/ IC_{50} of the tested compound against the cancer cell line.

Additionally, the ten compounds with the best IC_{50} values in the in vitro cell line screening were subjected to further in vitro VEGFR-2 inhibition screening in comparison with two reference drugs, Sorafenib and Sunitinib, with the results summarized in Table 1.

The results revealed that the tested compounds elicit a potent VEGFR-2 inhibitory activity in the submicromolar level. Compound **3j** showed superior VEGFR-2 inhibition (IC_{50} = 0.07 μM) than that displayed by Sunitinib (IC_{50} = 0.12 μM) and nearly equal to that of Sorafenib (IC_{50} = 0.06 μM). Six compounds (**3c**, **3f**, **3g**, **3h**, **3i**, and **6i**) showed nearly equipotent VEGFR-2 inhibition (IC_{50} = 0.10−0.16 μM) to Sunitinib (IC_{50} = 0.12 μM) but less than Sorafenib (IC_{50} = 0.06 μM). The structure−activity relationship (SAR) studies revealed that the *N*-substituted thiazole derivative **6i** among the ester series was the most active with an IC_{50} value of 0.11 μM. Moreover, the 4-chloro phenyl derivatives in the first imidazolone series (**3f**, **3h**, and **3i**) showed considerable inhibitory activity against VEGFR-2 with IC_{50} values of 0.10, 0.11, and 0.10 μM, respectively. Among all the tested compounds, the diazino-substituted derivative **3j** displayed the better activity against VEGFR-2 with an IC_{50} value of 0.07 μM compared to Sunitinib (IC_{50} = 0.12 μM), and was moderately less active than Sorafenib (IC_{50} = 0.06 μM).

The effect of compound **3j** on different cell cycle phases of the MCF7 cell line was examined by flow cytometric analysis. The results are displayed in Figure 3, showing that exposure of MCF7 cells to compound **3j** resulted in G1 apoptosis of 22.68% of cells compared to the control, which showed apoptosis of 11.07%. Likewise, the results also revealed significant arrest of the cell cycle at G2−M phases for **3j** (35.17%) compared to control (13.52%). Furthermore, the apoptotic effect of compound **3j** was studied using Annexin-V FTIC/PI dual staining assay at its IC_{50} on the MCF7 cancer cell line. This result demonstrated an increase in the percentage of early and late apoptotic cells (right bottom + right top), from 0.06% to 22.84% and from 0.68% to 42.21%, respectively. Finally, it revealed an 82-fold increase in the necrotic ability (left top) against the MCF7 cell line (1.64%) compared to the control (0.02%), as shown in Figure 3.

Antiproliferative activity against human umbilical vein endothelial cells (HUVEC) analysis was undertaken and selected to imitate proliferating neovasculature in order to evaluate the angiogenic inhibitory activity of the most promising compound, **3j**, in the in vitro VEGFR-2 kinase

https://doi.org/10.1021/acsmedchemlett.4c00095
ACS Med. Chem. Lett. 2024, 15, 892−898

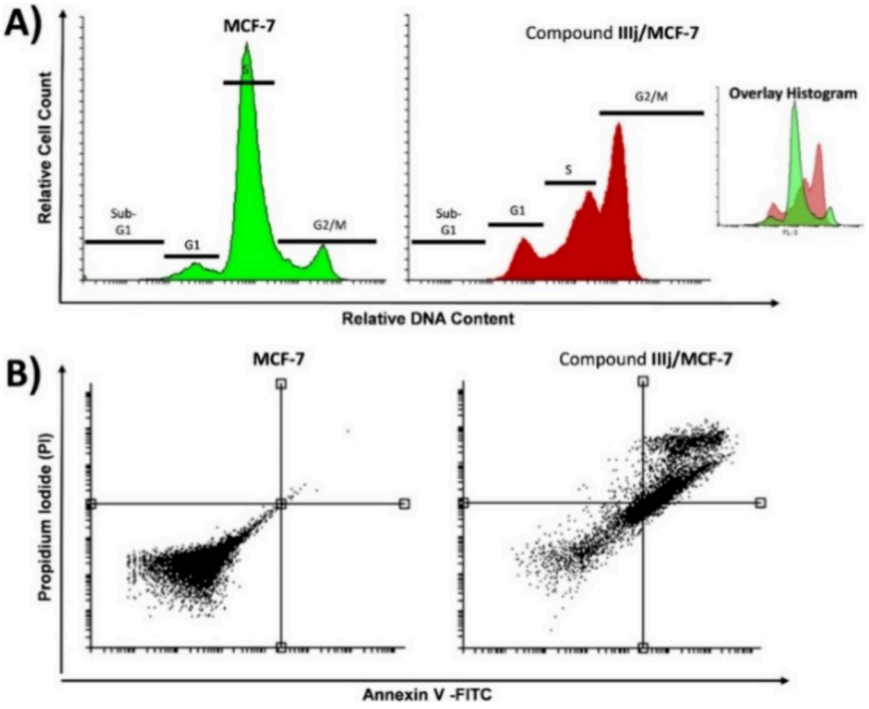

Figure 3. Flow cytometric analysis of cell cycle phases and apoptosis. (A) The representative histograms show the cell cycle distribution of the control (MCF-7) and cells treated with 5.86 μM (IC_{50} value) of compound **3j** for 72 h. (B) Flow cytometric charts of apoptosis in MCF-7 cells exposed to compound **3j** (5.86 μM) for 72 h.

assay.[23] Compound **3j** was subjected to an MTT assay against HUVEC using Sorafenib as a positive control. Results were expressed as IC_{50} (μM) ± standard deviation (SD) in Table 3.

Table 3. IC_{50} Values in μM of Compound 3j and Sorafenib on Human Umbilical Vein Endothelial Cells (HUVEC)

Compound	IC50 (μM)
3j	178.7 ± 7.71
Sorafenib	89.77 ± 3.87

The results revealed that an almost doubled concentration of compound **3j** relative to Sorafenib is required to produce the desired antiproliferative activity, indicating its safety as indicated from their IC_{50} values (IC_{50} = 178.7 and 89.77 μM, respectively).

Additionally, cell invasion and migration analysis was carried out using the scratch-wound assay, which measures the migratory rate of investigated cells where migratory cells are able to extend protrusions and ultimately invade and close the induced wound field.[24] A scratch assay of compound **3j** on HUVEC exhibited remarkable migration inhibitory ability relative to the control and was comparable relative to Sorafenib, as indicated from their wound closure percentage (65.93%, 97.04%, and 57.04%, respectively), as shown in Table 4.

Molecular docking was performed for compounds **3j** and **3i**, which showed significant VEGFR-2 inhibitory activity, to demonstrate the interaction of the newly synthesized compounds with the VEGFR-2 kinase domain, the rationale of their biological activity, and their possible binding pattern. The protein structure used for the docking studies was the crystal structure of the VEGFR-2 kinase domain in complex with a pyrazolone inhibitor (PDB code: 3U6J).[25] The structure has a resolution of 2.15 Å and a novel type II pyrazolone

Table 4. Migration Inhibition Percentage as Reflected from the Field Closure Percentage of Compound 3j, Sorafenib, and the Control by Wound Scratch Assay

Compound	Field closure percentage
3j	65.926
Sorafenib	57.037
Control	97.037

inhibitor cocrystallized in the binding pocket of the enzyme. The validation of the docking protocol was carried out by the redocking of the cocrystallized ligand and resulted in an RMSD value of 0.309 Å, shown in Figure 4a. Both compounds **3j** and **3i** form a hydrogen bond with Cys-919 in the hinge region, and the imidazolone moiety is surrounded with a hydrophobic region composed of Leu-840, Phe-918, and Gly-922, as shown in Figures 4b, c. The full list of interactions formed between the compounds and the binding site of the enzyme are listed in the Supplementary Data.

To further investigate the stability of the binding pose of compound **3j**, a 30 ns molecular dynamics simulation was carried out. The visual inspection of the trajectory of the protein−ligand complex generated from the simulation over a period of 30 ns showed the stability of the selected binding pose in the pocket of the protein. Moreover, the fluctuations of the position of the atoms of both the protein and the ligand were monitored across the molecular simulation run through the calculation of the RMSD values for the position of the atoms. The RMSD trajectories for the protein fluctuated between a minimum of 0.1 to 0.25 nm with an average of 0.17 nm. On the other hand, the fluctuations for the RMSD values for the ligand ranged between 0.05 and 0.14 nm, with an average of 0.1 nm. The low values of the RMSD confirm the stability of the selected pose in the binding pocket. Additionally, the number of hydrogen bonds formed between

https://doi.org/10.1021/acsmedchemlett.4c00095
ACS Med. Chem. Lett. 2024, 15, 892−898

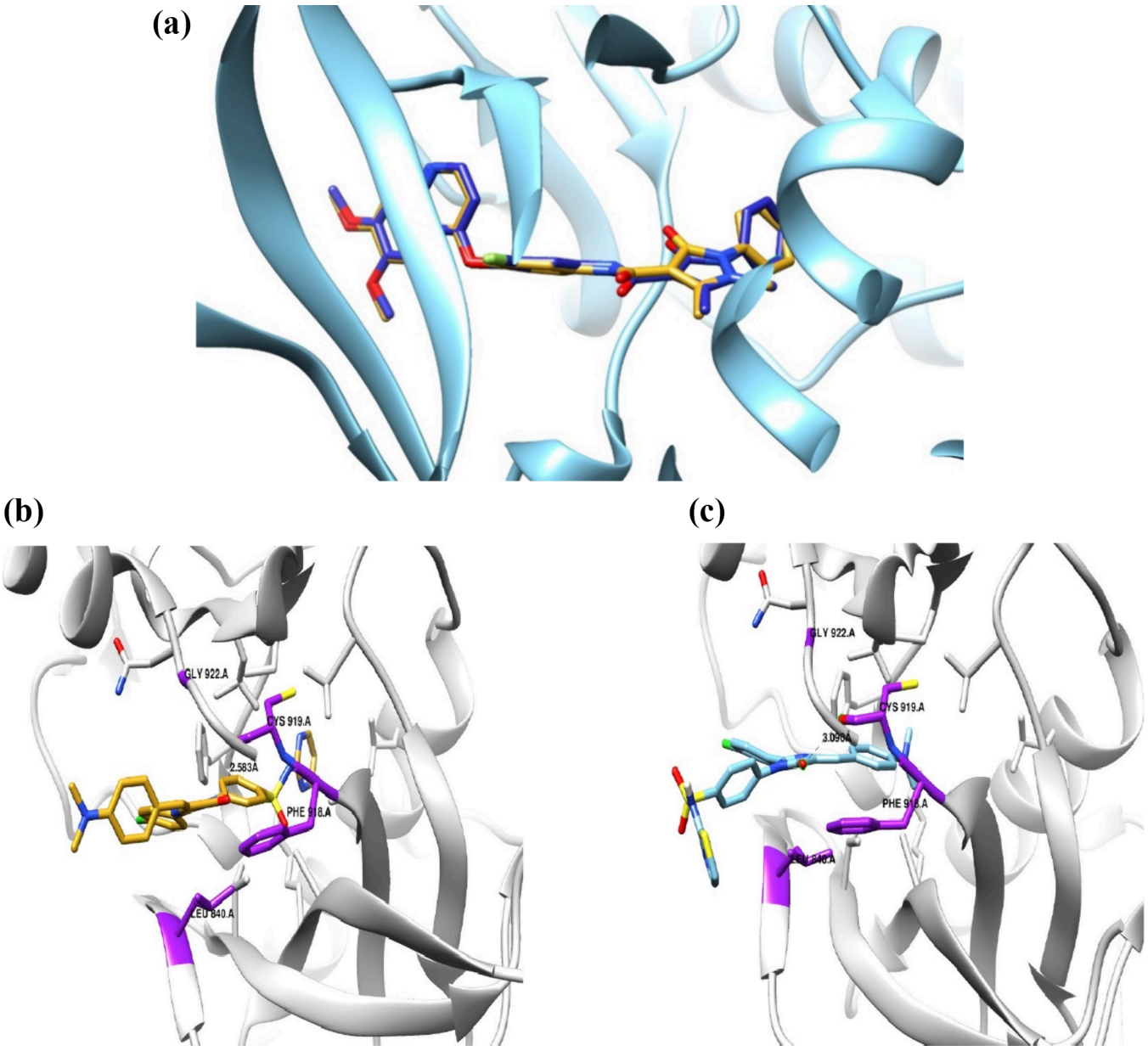

Figure 4. (a) The cocrystallized ligand (shown in blue) and the redocked ligand (shown in yellow). The best docked pose of compounds **3j** (b) and **3i** (c) into the binding pocket of the VEGFR enzyme, with key interacting residues are shown in purple.

the protein and the ligand were monitored over the molecular dynamics simulation. The average number of hydrogen bonds formed was found to be 2.

In summary, 20 new 1,2,4-trisubstituted imidazolones were synthesized, and their structures were elucidated using microanalyses and different spectral data. All compounds were examined for their in vitro anticancer activities against human breast (MCF-7) and lung (A549) cancer cell lines. Compound **3j** showed a superior IC_{50} value (IC_{50} = 5.86 μM) compared to the positive control (Doxorubicin) with an IC_{50} value of 6.52 μM against the MCF-7 cell line. The ten most active compounds were tested for their VEGFR-2 inhibitory activity, and again, compound **3j** showed superior activity against the VEGFR-2 kinase enzyme (IC_{50} = 0.07 μM) in comparison to the reference, Sunitinib (IC_{50} = 0.12 μM). In addition, compounds **3f**, **3h**, **3i**, and **6i** also elicited high activity against this enzyme with IC_{50} values of 0.10, 0.11, 0.10, and 0.11 μM, respectively. Moreover, compound **3j** was subjected to cell cycle analysis on the MCF-7 cell line, where it produced a G1 apoptosis percentage of 22.68% compared to the control (11.07%). Besides, it also resulted in a significant arrest of the cell cycle at G2−M phases of 35.17% compared to the control (13.52%). Additionally, HUVEC analysis carried out on compound **3j** to confirm antiproliferative potential required double the concentration when compared to the reference standard, Sorafenib, indicating its higher safety potential. Moreover, compound **3j** exhibited migration inhibitory ability higher than the control and comparable to that of Sorafenib. Also, molecular docking and dynamic studies were carried out to predict and confirm the stability of the binding pose of compound **3j**, as well as to predict its possible binding interactions. These results suggest that compound **3j** is a possible anticancer candidate via VEGFR-2 inhibition.

https://doi.org/10.1021/acsmedchemlett.4c00095
ACS Med. Chem. Lett. 2024, 15, 892−898

■ ASSOCIATED CONTENT

Supporting Information

The Supporting Information is available free of charge at https://pubs.acs.org/doi/10.1021/acsmedchemlett.4c00095.

Additional experimental procedures, biological assays, and in silico studies (PDF)

■ AUTHOR INFORMATION

Corresponding Authors

Walaa R. Mahmoud − *Department of Pharmaceutical Chemistry, Faculty of Pharmacy, Cairo University, Cairo 11562, Egypt*; Phone: +2 01001518979; Email: walaa.abozaid@pharma.cu.edu.eg

Rana H. Refaey − *Pharmaceutical Chemistry Department, Faculty of Pharmacy, October University for Modern Sciences and Arts (MSA), Giza 12411, Egypt*; orcid.org/0000-0003-3794-9116; Phone: +2 01223179426; Email: rhosny@msa.edu.eg

Authors

Manar R. Mohamed − *Department of Pharmaceutical Chemistry, Faculty of Pharmacy, Cairo University, Cairo 11562, Egypt*

Riham F. George − *Department of Pharmaceutical Chemistry, Faculty of Pharmacy, Cairo University, Cairo 11562, Egypt*

Hanan H. Georgey − *Department of Pharmaceutical Chemistry, Faculty of Pharmacy, Cairo University, Cairo 11562, Egypt; Department of Pharmaceutical Chemistry, Faculty of Pharmacy and Drug Technology, Egyptian Chinese University, Cairo 19346, Egypt*

Complete contact information is available at: https://pubs.acs.org/10.1021/acsmedchemlett.4c00095

Notes

The authors declare no competing financial interest.

■ REFERENCES

(1) Sakkiah, S.; Cao, G.P.; Gupta, S.P.; Lee, K.W. Overview of the Structure and Function of Protein Kinases. *Current Enzyme Inhibition* **2017**, *13*, 81.

(2) Morabito, A.; De Maio, E.; Di Maio, M.; Normanno, N.; Perrone, F. Tyrosine Kinase Inhibitors of Vascular Endothelial Growth Factor Receptors in Clinical Trials: Current Status and Future Directions. *Oncologist* **2006**, *11*, 753−764.

(3) Álvarez-Aznar, A.; Muhl, L.; Gaengel, K. VEGF Receptor Tyrosine Kinases. *Curr Top Dev Biol* **2017**, *123*, 433−482.

(4) Shibuya, M. Vascular Endothelial Growth Factor (VEGF) and Its Receptor (VEGFR) Signaling in Angiogenesis: A Crucial Target for Anti- and Pro-Angiogenic Therapies. *Genes & Cancer* **2011**, *2* (12), 1097−1105.

(5) Carmeliet, P. VEGF as a Key Mediator of Angiogenesis in Cancer. *Oncology* **2005**, *69*, 4−10.

(6) Roskoski, R. Classification of small molecule protein kinase inhibitors based upon the structures of their drug-enzyme complexes. *Pharmacol. Res.* **2016**, *103*, 26−48.

(7) Mourad, A. A. E.; Farouk, N. A.; El-Sayed, E.-S. H.; Mahdy, A. R. E. EGFR/VEGFR-2 dual inhibitor and apoptotic inducer: Design, synthesis, anticancer activity and docking study of new 2-thioxoimidazolidin-4one derivatives. *Life Sciences* **2021**, *277*, 119531.

(8) Kiselyov, A. S.; Semenova, M.; Semenov, V. V. Hetaryl imidazoles: A novel dual inhibitors of VEGF receptors I and II. *Bioorg. Med. Chem. Lett.* **2006**, *16*, 1440−1444.

(9) El-Hady, H. A.; Abubshait, S. A. Synthesis and anticancer evaluation of imidazolinone and benzoxazole derivatives. *Arabian Journal of Chemistry* **2017**, *10*, S3725−S3731.

(10) Ramaiah, M. J.; Pushpavalli, S.; Krishna, G. R.; Sarma, P.; Mukhopadhyay, D.; Kamal, A.; Bhadra, U.; Bhadra, M. P. Chalcone-imidazolone conjugates induce apoptosis through DNA damage pathway by affecting telomeres. *Cancer Cell International* **2011**, *11*, 11.

(11) ElSayed, S.; ElAshmawy, M.; Bayoumi, S.; Hassan, G.; ElSubbagh, H. New Imidazole-4-one and Imidazolidine-2,4-dione Analogues: Design, Synthesis, Antitumor activity and Molecular Modeling Study. *American Journal of Physiology, Biochemistry and Pharmacology* **2018**, *7*, 24.

(12) casini, A.; Scozzafava, A.; Mastrolorenzo, A.; Supuran, C. Sulfonamides and Sulfonylated Derivatives as Anticancer Agents. *Current Cancer Drug Targets* **2002**, *2*, 55−75.

(13) Ghorab, M. M.; Ragab, F. A.; Hamed, M. M. Design, synthesis and anticancer evaluation of novel tetrahydroquinoline derivatives containing sulfonamide moiety. *Eur. J. Med. Chem.* **2009**, *44*, 4211−4217.

(14) Ghorab, M.M.; Ragab, F.A.-F.; Heiba, H.I.; Agha, H. Synthesis of Some Novel Sulfonamides Containing Biologically Active Alkanoic Acid, Acetamide, Thiazole, and Pyrrole Moieties of Expected Antitumor and Radiosensitizing Activities. *J. Basic Appl. Chem.* **2011**, *1* (2), 8−14.

(15) Tandel, R. C.; Mammen, D. Synthesis and study of some compounds containing oxazolone ring, showing biological activity. *Ind.j.Chem.- Sec. B Org. Med. Chem.* **2008**, *47*, 932−937.

(16) Kuş, C.; Uğurlu, E.; Özdamar, E. D.; Can-Eke, B. Yeni oksazol-5(4H)-one türevlerinin sentez ve antioksidan özellikleri. *Turk J. Pharm. Sci.* **2017**, *14*, 174−178.

(17) Karale, B. K.; Gadhave, A. G. Synthesis and antibacterial activity of some spiroisoxazolines. *Ind. Journal of Heterocyclic Chemistry* **2010**, *19*, 389−392.

(18) Abdel Gawad, N. M.; Amin, N. H.; Elsaadi, M. T.; Mohamed, F. M.M.; Angeli, A.; De Luca, V.; Capasso, C.; Supuran, C. T. Synthesis of 4-(thiazol-2-ylamino)-benzenesulfonamides with carbonic anhydrase I, II and IX inhibitory activity and cytotoxic effects against breast cancer cell lines. *Bioorg. Med. Chem.* **2016**, *24*, 3043−3051.

(19) Georgey, H. H.; Manhi, F. M.; Mahmoud, W. R.; Mohamed, N. A.; Berrino, E.; Supuran, C. T. 1,2,4-Trisubstituted imidazolinones with dual carbonic anhydrase and p38 mitogen-activated protein kinase inhibitory activity. *Bioorganic Chemistry* **2019**, *82*, 109−116.

(20) Awadallah, F. M.; Bua, S.; Mahmoud, W. R.; Nada, H. H.; Nocentini, A.; Supuran, C. T. Inhibition studies on a panel of human carbonic anhydrases with *N* 1-substituted secondary sulfonamides incorporating thiazolinone or imidazolone-indole tails. *Journal of Enzyme Inhibition and Medicinal Chemistry* **2018**, *33*, 629−638.

(21) Ghorab, M. M.; Ragab, F. A.; Heiba, H. I.; El-Hazek, R. M. Anticancer and radio-sensitizing evaluation of some new thiazolopyrane and thiazolopyranopyrimidine derivatives bearing a sulfonamide moiety. *Eur. J. Med. Chem.* **2011**, *46*, 5120−5126.

(22) Saeedi, M.; Goli, F.; Mahdavi, M.; Dehghan, G.; Faramarzi, M. A.; Foroumadi, A.; Shafiee, A. Synthesis and biological investigation of some novel sulfonamide and amide derivatives containing coumarin moieties. *Iranian Journal of Pharmaceutical Research: IJPR* **2014**, *13*, 881.

(23) Jie, S.; Li, H.; Tian, Y.; Guo, D.; Zhu, J.; Gao, S.; Jiang, L. Berberine inhibits angiogenic potential of Hep G2 cell line through VEGF down-regulation in vitro. *Journal of Gastroenterology and Hepatology (Australia)* **2011**, *26*, 179.

(24) Cory, G. Scratch-Wound Assay. *Methods Mol. Biol.* **2011**, *769*, 25−30.

(25) Norman, M.H.; Liu, L.; Lee, M.; Xi, N.; Fellows, I.; D'Angelo, N. D.; Dominguez, C.; Rex, K.; Bellon, S.F.; Kim, T.S.; Dussault, I. Structure-based design of novel class II c-Met inhibitors: 1. Identification of pyrazolone-based derivatives. *J. Med. Chem.* **2012**, *55*, 1858.